Article

Comparison of HO/UV and Heterogeneous Photocatalytic Processes for the Degradation of Dichloroacetic Acid In Water

C. S. Zalazar, M. L. Satuf, O. M. Alfano, and A. E. Cassano

Environ. Sci. Technol., **2008**, 42 (16), 6198-6204• DOI: 10.1021/es800028h • Publication Date (Web): 12 July 2008

Environ. Sci. Technol. **2008,** *42,* 6198–6204

Comparison of H_2O_2/UV and Heterogeneous Photocatalytic Processes for the Degradation of Dichloroacetic Acid In Water

C. S. ZALAZAR, M. L. SATUF, O. M. ALFANO, AND A. E. CASSANO*

INTEC (Universidad Nacional del Litoral and CONICET), Güemes 3450 (3000), Santa Fe, Argentina

Received February 14, 2008. Revised manuscript received May 3, 2008. Accepted May 8, 2008.

A comparative study between two advanced oxidation technologies for pollutant degradation has been made. With the use of dichloroacetic acid (DCA) as the model pollutant, the reactions with hydrogen peroxide and UV radiation (H_2O_2/UV, 253.7 nm) and photocatalysis with titanium dioxide (TiO_2/UV, 300−400 nm) are analyzed. Three criteria have been selected to compare the performances of both processes: (i) the percentage conversion of DCA and TOC (total organic carbon) at a fixed reaction time; (ii) the quantum efficiency, employing the true radiation absorption rates for both activated species (H_2O_2 and TiO_2); (iii) the specific energy consumption to degrade 50% of the initial TOC. The optimal molar concentration ratio of H_2O_2/DCA and the optimal catalyst concentration have been employed in the experiments. The results indicate that, under the optimal operating conditions, the H_2O_2/UV process exhibits, by a large difference, the best performance taking into account the above-mentioned criteria. Nevertheless, both systems show similar values of specific energy consumption when a thinner reactor is employed. These results cannot be safely extrapolated to other contexts if (i) other compounds of different structure are degraded and (ii) a different catalyst is used. Moreover, they were obtained under optimized conditions, and typical, real-life situations may render quite different results due to the robustness of the titanium dioxide operation. They should serve as an indication that, under the studied conditions, a much-improved catalyst performance must be achieved to parallel, with a heterogeneous process, a yield similar to the one obtained with the homogeneous system.

Introduction

Advanced oxidation technologies (AOT) constitute a family of destructive processes that have been successfully employed to degrade organic pollutants in water. One particular subset of these methods uses UV radiation as the source of external energy. Among them, titanium dioxide and UV (TiO_2/UV) (*1–3*), hydrogen peroxide and UV (H_2O_2/UV) (*4–6*), and the photo-Fenton reaction (H_2O_2/Fe^{3+}/UV) (*7–9*) are the most widely employed. Our group has studied two of these processes (TiO_2/UV and H_2O_2/UV) employing the same model compound: dichloroacetic acid (DCA) (*10–13*). Studies on the photocatalytic activity of titanium dioxide to degrade DCA can also be found in the literature (*14, 15*). DCA is a pollutant that can be found in water as a result of chlorine disinfection. In addition, DCA can be detected in wastewaters resulting from the degradation of chlorinated compounds such as trichloroacetic acid, perchloroethylene, and trichloroethylene (*16*).

In the contributions previously referenced (*10–13*), the reaction kinetics for the two processes were analyzed and two different models were used based on plausible and almost complete reaction mechanisms. These models were validated with experiments. However, the employed experimental conditions in the photocatalytic reaction and in the H_2O_2/UV reaction, particularly the lamps nominal input power, were so different that a fair comparison was almost impossible. Thus in this work, the operating conditions were adjusted to permit a measurable and objective comparison between both reactions. Three different criteria were used to contrast both processes: (i) the DCA and TOC conversion at a chosen, fixed irradiation time, (ii) the quantum efficiency, and (iii) the specific energy consumption (i.e., amount of energy consumed to remove 50% of the initial TOC concentration). The definition of each one of these criteria will be discussed along the present contribution.

An important point should be noted beforehand. Aldrich titanium dioxide has been selected as the catalyst for the heterogeneous process because it causes minimal fouling of the reactor windows. Other more active catalysts, like the well-known Degussa P 25, could have been used, but they usually originate important fouling of the windows and turn invalid the value of the boundary conditions employed in the modeling of the radiation field (*17*). Consequently, results obtained in this work cannot be fully generalized and are strictly valid for the Aldrich catalyst.

Experimental Setups and Procedures

Both oxidation processes were carried out in small reactors that operate in a recirculation batch mode.

Hydrogen Peroxide/UV Radiation Process. The reacting system has five sections: (i) the reactor, (ii) the recirculating pump, (iii) the storage tank, (iv) the heat exchanger, and (v) the irradiation system. The reactor was a cylinder made of Teflon closed in both extremes with two demountable, flat, circular windows made of quartz of Suprasil quality. The reactor length was 5.2 cm, and the volume was 110 cm^3. The tank was equipped with a sampling valve and a port for temperature measurements. The volume of the solution in the tank plus the reactor volume (V_R) and the connecting lines (including the pump and the heat exchanger) totaled a volume of 3000 cm^3 (V_T). Radiation energy was supply by two lamps (one on each side of the windows) located vertically at the focal axis of their respective custom-made parabolic reflectors. Two different types of lamps were used: (1) two Philips TUV lamps having an input power of 15 W each and (2) two Heraeus UV-C lamps operated with an input power of 40 W each. Both types of lamps are low-pressure mercury vapor lamps (germicidal type) with one single significant emission wavelength at 253.7 nm. The photoreactor, the reflectors, and the UV lamps were enclosed in a box to ensure safe operation and to prevent the entrance of extraneous light. Good mixing in the reactor was surely achieved by means of an intense recirculation of the liquid.

DCA and chloride ion were analyzed in a Dionex ion chromatograph (Dionex 2020i). H_2O_2 was analyzed with a spectrophotometric method at 350 nm according to Allen et al. (*18*), employing a Cary 100 Bio UV−vis instrument. Total

* Corresponding author fax: 54-342-4511087; e-mail: acassano@santafe-conicet.gov.ar; phone: 54-342-4511370/72/73 ext. 1066.

10.1021/es800028h CCC: $40.75
Published on Web 07/12/2008

TABLE 1. Experimental Conditions

variable	process	
	H_2O_2/UV	TiO_2/UV
DCA concentration	60 ppm	60 ppm
radiation absorbing species concentration	H_2O_2: 145 ppm	TiO_2: 1.0×10^{-3} g cm^{-3}
lamp	Heraeus UVC 40 W and Philips TUV 15 W on each side.	Philips black light TL 4W/08 4 on each side
lamp emission	253.7 nm spectral line, voluminal	300−400 nm, peak at 350 nm continuous, superficial
$G_{W,\lambda}$ or $G_{W,\Sigma\lambda}$	29.8×10^{-9} einstein cm^{-2} s^{-1} (40 W each side) 9.94×10^{-9} einstein cm^{-2} s^{-1} (15 W each side)	7.55×10^{-9} einstein cm^{-2} s^{-1} (16 W each side)
pH	3.4 (natural)	4.0 (natural)
temp	20 °C	20 °C

organic carbon (TOC) was also analyzed (Shimadzu TOC-5000A) in order to compare the degradation rate of DCA with the total mineralization rate. pH was controlled with an Orion EA 940 pH meter.

Further details on the experimental device, reactants, and procedure can be found elsewhere (*12*).

Titanium Dioxide/UV Radiation Process. The reacting system has five sections: (i) the reactor, (ii) the recirculating pump, (iii) the storage tank, (iv) the oxygen bubbling system, and (v) the irradiation system. The reactor was a cylindrical tube made of Teflon with an external clad made of stainless steel. The length of the reactor was 5 cm, and the internal radius was 4.3 cm, totaling a reactor volume of 290 cm^3 (V_R). The reactor had two flat, circular windows made of borosilicate glass. Ground borosilicate glasses were situated at the external side of both windows in order to produce diffuse incoming radiation. The pump flow rate was adjusted to provide good mixing conditions, low conversion per pass in the reactor, and uniform concentration of the catalyst throughout the system. The tank included provisions for sampling and temperature measurements. It was surrounded by a water circulating jacket to ensure isothermal conditions during the reaction time. The volume of the solution in the tank plus the one of the reactor and the connecting lines (including the pump) totaled a volume of 1000 cm^3 (V_T). An oxygen bubbling system with a glass disperser operated continuously in the tank to maintain constant the gas concentration in the reactor feed. Four 4 W, tubular black light lamps, placed in a box, were located on each side of the reactor windows. They were low-pressure UV A lamps from Philips (TL 4W/08) totaling an incoming power of 32 W. These lamps emitted in the range of 300−400 nm, having a peak at 350 nm. Samples taken from the tank were first centrifuged and then filtered to remove the catalytic particles before analyses.

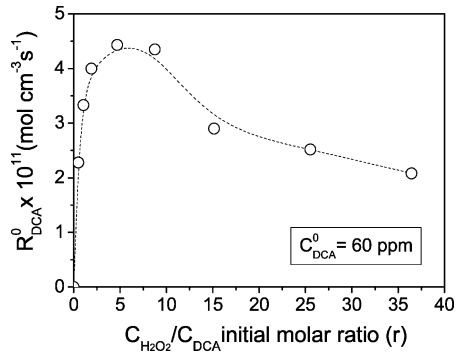

FIGURE 1. DCA initial reaction rate vs H_2O_2/DCA initial concentration ratios.

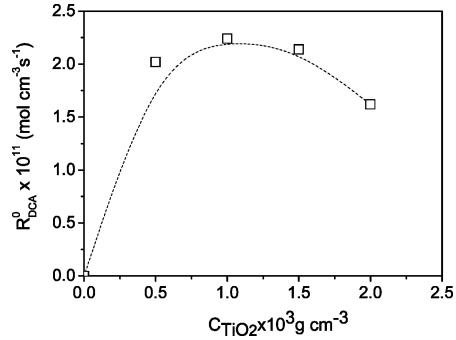

FIGURE 2. DCA initial reaction rate vs catalyst concentration.

TiO_2 powder (>99% anatase, 9.6 m^2 g^{-1} of specific surface area, 100−200 nm diameter of the elementary particles before agglomeration) was obtained from Aldrich Chemicals. Deionized water was used to prepare all solutions. Analyses of DCA, chloride ion, TOC, and pH were made as described in the previous section.

Preliminary Runs. Control experiments were made in both systems to ensure that no direct photolysis of DCA was produced. No evidence of DCA degradation was found in the absence of hydrogen peroxide or titanium dioxide. A second set of experiments was made to disregard direct oxidation by hydrogen peroxide. Results indicated that DCA degradation does not take place in the absence of UV radiation (*10, 12*).

Optimal Operating Conditions for Both Systems. Several studies carried out employing the H_2O_2/UV process have shown the existence of an optimal hydrogen peroxide concentration. The accepted explanation is that when the hydrogen peroxide concentration is too low the initiation rate is slow, mainly because absorption by H_2O_2 at 253.7 nm is rather weak. On the other hand, when the concentration of the oxidant is too large, it becomes a scavenger of ·OH radicals, competing with the pollutant degradation. It is clear that the H_2O_2 radiation absorption is the most significant variable influencing the reaction rate (*19, 20*). However, we have found that the initial ratio "*r*", defined as $r = C_{H_2O_2}/C_{DCA}$, modifies the optimal H_2O_2 concentration. Also, the magnitude of the optimal H_2O_2 concentration depends on the nature of the pollutant and should be experimentally verified (*21*).

Similarly, for the TiO_2/UV process, there is an optimal concentration of the catalyst that renders the highest reaction rates. Beyond a given catalyst concentration, two phenomena produce a decline in the reaction rate: (i) due to the high radiation absorption rate, convective motion inside the reactor can not compensate the increasing inability to activate all the catalytic particles in the whole reactor volume, and (ii) mass transport limitations start to play an active role in

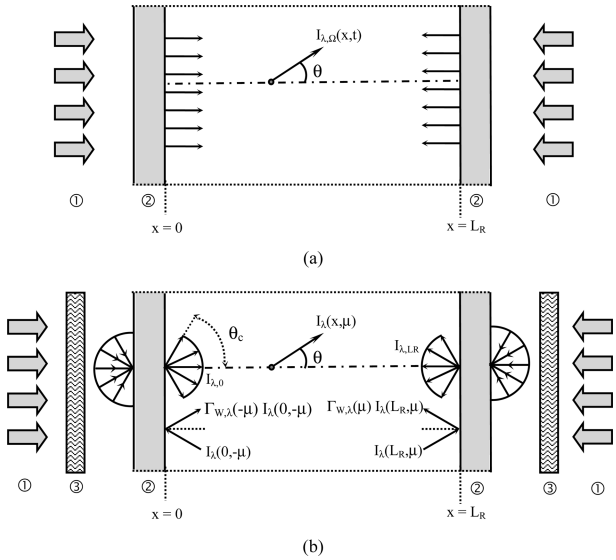

FIGURE 3. Reactor scheme including the coordinate system for the radiation model: (a) homogeneous reactor; (b) heterogeneous reactor. Keys: (1) radiation source, (2) reactor windows, (3) ground glass plates.

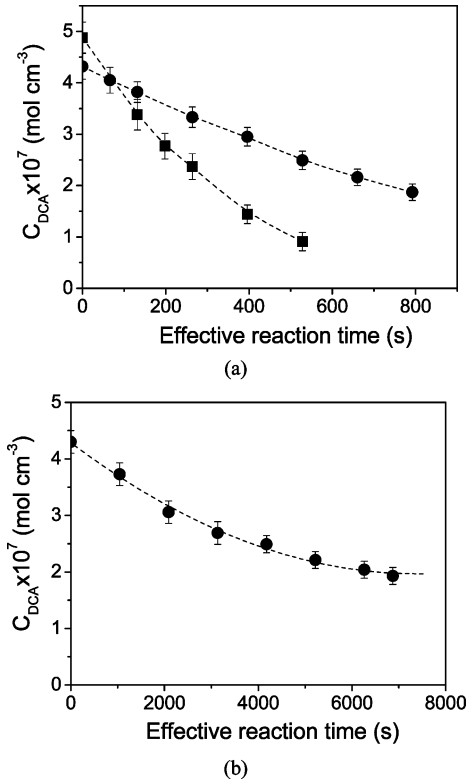

FIGURE 4. (a) DCA concentration vs effective reaction time for the H_2O_2/UV process and $C_{H_2O_2}/C_{DCA} = 8$. Keys: (●) 15 W lamps; (■) 40 W lamps. (b) DCA concentration vs effective reaction time for the TiO_2/UV process and $C_m = 1 \times 10^{-3}$ g cm^{-3}.

the reaction kinetics (*22*). The optimal concentration depends on the properties of the catalyst and on those of the chemical compound under analysis. It should be measured for each particular application.

Experimental runs were made with the H_2O_2/UV and TiO_2/UV systems to find the optimal conditions for the DCA degradation. In the first case, the analysis was aimed to obtain the best initial molar ratio "*r*" of $C_{H_2O_2}/C_{DCA}$. In the second case, experiments were made to find the best catalyst concentration, C_m, that remains constant throughout the runs. The operating conditions employed in the experiments are summarized in Table 1. The incident radiation rates at the reactor windows ($G_{W,\lambda}$ and $G_{W,\Sigma\lambda}$ for H_2O_2/UV and TiO_2/UV, respectively) were obtained with potassium ferrioxalate actinometry, and they were calculated according to Zalazar et al. (*23*).

Results are shown in Figures 1 and 2. It was concluded that $r = 3-10$ and $C_m = 1.0 \times 10^{-3}$ g cm^{-3} were the proper values to be used. Both values were obtained for an initial DCA concentration of 60 ppm.

Comparison Criteria

The following criteria were applied to compare both processes:

DCA and TOC Conversion after a Fixed Reaction Time. DCA conversion refers to the amount of reactant degraded at a defined reaction time. Also, to assess the mineralization of DCA, the TOC conversion was evaluated.

Quantum Efficiency. The proper determination of quantum yields and quantum efficiencies has been the subject of research by different groups (*24–36*).

The quantum yield (η_λ) is a property that can be used only for monochromatic radiation. Hence, it could be applied to the H_2O_2/UV reaction because almost monochromatic radiation was employed. The term quantum efficiency ($\eta_{\Sigma\lambda}$) has been suggested by Braun et al. (*24*) for those cases in which polychromatic radiation is used. The general definition of quantum efficiency (or quantum yield) can be written in the following way:

$$\eta_\lambda \quad \text{or} \quad \eta_{\Sigma\lambda} = \frac{\text{number of molecules of reactant disappeared or product formed in a given time } t}{\text{number of } \textbf{absorbed} \text{ photons by the species initiating the reaction in the same time t}} \tag{1}$$

In terms of rates, η_λ and $\eta_{\Sigma\lambda}$ can be defined as follows:

$$\eta_\lambda \quad \text{or} \quad \eta_{\Sigma\lambda} = \frac{\text{reaction rate of reactant disappeared or product formed}}{\text{photon } \textbf{absorption} \text{ rate by the specific radiation absorbing species}} \tag{2}$$

In this study, the specific radiation absorbing species are the hydrogen peroxide or the titanium dioxide catalyst, depending on the process under analysis.

In the above-mentioned references, several methods have been proposed to calculate η_λ or $\eta_{\Sigma\lambda}$. The majority of them produce an approximation to the value of the quantum efficiency because of unavoidable experimental restrictions in the characterization of light absorption with scattering (*25–27, 29–31*). A precise evaluation of radiation absorption can be obtained from the mathematical solution of the radiative transfer equation (RTE) (*28, 32, 35, 36*).

In the present approach, the denominator of eq 2 was calculated from the solution of the RTE employing the specific optical properties of the absorbing reactant or catalyst, respectively. The properties of the catalyst were obtained from especial spectrophotometric measurements (*37*).

Energy Consumption with Respect to the TOC Removed. Badawy et al. (*38*) defined the specific energy consumption (E_S) as the energy required by a photochemical process to remove 70% of the initial TOC present in an aqueous sample (kW h kg^{-1}). A modification of this criterion was used in the present work, where E_S is redefined as

$$E_S = \frac{P_{UV} t}{0.5[TOC_0] V_R}[=]\frac{W\ s}{kg} \tag{3}$$

This parameter represents the amount of energy (W s) required to remove 50% of the initial mass (kg) of TOC existing in the reactor. P_{UV} is the input power of the lamp (W), t (s) is the time required to remove 50% of the initial TOC concentration (kg m^{-3}), and V_R is the reactor volume (m^3).

Reaction Rate and Local Volumetric Rate of Photon Absorption

As stated previously, for the homogeneous reaction, the quantum efficiency is equal to the quantum yield because almost monochromatic radiation is used. Then, the following equation applies:

$$\eta_{i,\lambda}^{\mathrm{Hom}} = \frac{\left\langle R_i^{\mathrm{Hom}}(\mathbf{x}, t_0)\right\rangle_{V_R}}{\left\langle e_{H_2O_2,\lambda}^{a,\mathrm{Hom}}(\mathbf{x}, t_0)\right\rangle_{V_R}} \tag{4}$$

where i = DCA, TOC, $\langle R_i^{\mathrm{Hom}}(x,t_0)\rangle_{V_R}$ is the initial reaction rate averaged over the reactor volume, and $\langle e_{H_2O_2,\lambda}^{a,\mathrm{Hom}}(\mathbf{x},t_0)\rangle_{V_R}$ is the local volumetric rate of photon absorption (LVRPA) at initial conditions, averaged over the reactor volume.

For the heterogeneous catalytic reaction with polychromatic light, the following equation applies:

$$\eta_{i,\Sigma\lambda}^{\mathrm{Het}} = \frac{\left\langle R_i^{\mathrm{Het}}(\mathbf{x}, t_0)\right\rangle_{V_R}}{\left\langle e_{TiO_2,\Sigma\lambda}^{a,\mathrm{Het}}(\mathbf{x}, t_0)\right\rangle_{V_R}} \tag{5}$$

Reaction Rate. Considering the following assumptions, (i) the reactor and tank are very well mixed, (ii) the conversion per pass in the reactor is very small (differential), (iii) the ratio $V_R/V_T < 1$, and (iv) there is no direct photolysis, the mass balance for DCA in the homogeneous and heterogeneous systems results (*39, 40*):

$$\varepsilon_L \frac{dC_{DCA}(t)}{dt}_{Tk} = \frac{V_R}{V_T}\langle R_{DCA}(\mathbf{x}, t)\rangle_{V_R} \tag{6}$$

where ε_L is the liquid holdup, and the initial condition is $C_{DCA}(t_0) = C_{DCA}^0$. For the homogeneous system, $\varepsilon_L = 1$.

As the reactor operates in recirculation mode, we can define the effective time of exposure to radiation of the reacting mixture as

$$t_{eff} = \frac{V_R}{\varepsilon_L V_T} t \tag{7}$$

From eqs 6 and 7 results

$$\frac{dC_{DCA}(t_{eff})}{dt_{eff}}_{Tk} = \langle R_{DCA}(\mathbf{x}, t_{eff})\rangle_{V_R} \tag{8}$$

The initial reaction rate can be calculated from eq 8 as

$$\langle R_{DCA}(\mathbf{x}, t_{eff,0})\rangle_{V_R} = \lim_{t_{eff}\to t_{eff,0}}\left[\frac{C_{DCA}(t_{eff,0}) - C_{DCA}(t_{eff})}{t_{eff} - t_{eff,0}}\right]_{Tk} \tag{9}$$

Similarly, the initial rate of TOC degradation yields

$$\langle R_{TOC}(\mathbf{x}, t_{eff,0})\rangle_{V_R} = \lim_{t_{eff}\to t_{eff,0}}\left[\frac{C_{TOC}(t_{eff,0}) - C_{TOC}(t_{eff})}{t_{eff} - t_{eff,0}}\right]_{Tk} \tag{10}$$

Local Volumetric Rate of Photon Absorption. *Homogeneous Radiation Field.* From eq S1 (Supporting Information), for a homogeneous medium and a one-dimensional model, the following equation applies (Figure 3a) (*41*):

$$\mu\frac{dI_\lambda(x,\mu,t)}{dx} = -\kappa_\lambda(x,t) I_\lambda(x,\mu,t) \tag{11}$$

The variable μ represents cos θ. It has been shown that for one-dimensional and single-directional radiation propagation (*23*)

$$G_\lambda(x,t) = \tilde{I}_\lambda(x,t) \tag{12}$$

where $\tilde{I}_\lambda$ is a special specific intensity. Then, the RTE can be written as

$$\frac{dG_\lambda(x,t)}{dx} = -\kappa_\lambda(x,t) G_\lambda(x,t) \tag{13}$$

As the homogeneous reactor is irradiated from both sides, we can define

$$G_\lambda(x,t) = G_\lambda^I(x,t) + G_\lambda^{II}(x,t) \tag{14}$$

where G_λ^I is the incident radiation entering at $x = 0$ and G_λ^{II} is the incident radiation entering at $x = L_R$. Integrating eq 13 gives

$$G_\lambda^I(x,t) = G_{W,\lambda}^I \exp[-\kappa_\lambda(x,t)x] \tag{15}$$

$$G_\lambda^{II}(x,t) = G_{W,\lambda}^{II} \exp[-\kappa_\lambda(x,t)(L_R - x)] \tag{16}$$

where $G_{W,\lambda}^I$ and $G_{W,\lambda}^{II}$ are the boundary conditions at $x = 0$ and $x = L_R$, respectively. Considering $G_{W,\lambda}^I = G_{W,\lambda}^{II} = G_{W,\lambda}$, introducing eqs 15 and 16 into eq 14, and calculating the LVRPA with eq S3, results

$$e_{H_2O_2,\lambda}^a(x,t) = \kappa_{H_2O_2,\lambda}(t) G_{W,\lambda}\{\exp[-\kappa_{H_2O_2,\lambda}(t)x] + \exp[-\kappa_{H_2O_2,\lambda}(t)(L_R - x)]\} \tag{17}$$

In eq 17, it has been assumed that the only species that absorbs radiation is H_2O_2 and that, due to the prevailing mixing conditions, the absorption coefficient is not a function of the position ($\kappa_\lambda(x,t) = \kappa_{H_2O_2,\lambda}(t)$).

The volume average value of the LVRPA for the one-dimensional model results in an average taken along the x-direction:

$$\left\langle e_{H_2O_2,\lambda}^a(x,t)\right\rangle_{L_R} = \frac{2G_{W,\lambda}}{L_R}\{1 - \exp[-\kappa_{H_2O_2,\lambda}(t)L_R]\} \tag{18}$$

Heterogeneous Radiation Field. The reactor can be considered a one-dimensional reactor formed by two parallel flat plates. The diffuse radiation permits to consider that the radiation field has azimuthal symmetry, and consequently, the reactor behaves as a one-dimensional−one-directional system, as shown in Figure 3b. Under these conditions, eq S1 simplifies to (*42*)

$$\mu\frac{dI_\lambda(x,\mu)}{dx} + \beta_{TiO_2,\lambda} I_\lambda(x,\mu) = \frac{\sigma_{TiO_2,\lambda}}{2}\int_{\mu'=-1}^{1} I_\lambda(x,\mu') p(\mu,\mu')\, d\mu' \tag{19}$$

The phase function used for scattering was the Henyey and Greenstein phase function (*43*). The extinction coefficient is defined as $\beta_{TiO_2,\lambda} = \kappa_{TiO_2,\lambda} + \sigma_{TiO_2,\lambda}$. Assuming that the only species that absorbs radiation in the 300−400 nm wavelength range is the catalyst and that it is mechanically and chemically stable, in a well-mixed reactor $\beta_{TiO_2,\lambda}$, $\kappa_{TiO_2,\lambda}$, and $\sigma_{TiO_2,\lambda}$ are not a function of x or t.

The boundary conditions of eq 19 take into account that there is absorption, refraction, and reflection in the reactor windows:

$$I_\lambda(0,\mu) = I_{\lambda,0} + \Gamma_{\lambda,W}(-\mu) I_\lambda(0,-\mu) \qquad 1 \ge \mu \ge \mu_c \tag{20a}$$

$$I_\lambda(0,\mu) = \Gamma_{\lambda,W}(-\mu) I_\lambda(0,-\mu) \qquad \mu_c > \mu \ge 0 \tag{20b}$$

$$I_\lambda(L_R,-\mu) = I_{\lambda,L_R} + \Gamma_{\lambda,W}(\mu) I_\lambda(L_R,\mu) \qquad 1 \ge \mu \ge \mu_c \tag{20c}$$

$$I_\lambda(L_R, -\mu) = \Gamma_{\lambda,W}(\mu) I_\lambda(L_R, \mu) \qquad \mu_c > \mu \geq 0 \qquad (20d)$$

where $\mu_c = \cos\theta_c$. The detailed derivation of these boundary conditions can be found in Satuf et al. (*35*).

The numerical solution of eq 19, with the corresponding boundary conditions, was obtained with the discrete ordinate method (DOM) taken from Duderstadt and Martin (*44*). It must be noted that besides the spatial and directional discretizations in the DOM, a third discretization is needed for the λ-distribution of the employed wavelength range between 300 nm $\leq \lambda \leq$ 400 nm.

Considering azimuthal symmetry and polychromatic radiation, the LVRPA can be calculated with the following equation:

$$e^a_{TiO_2,\Sigma\lambda}(x) = 2\pi \int_\lambda \kappa_{TiO_2,\lambda} \int_{\mu=-1}^{1} I_\lambda(x,\mu)\, d\mu\, d\lambda \qquad (21)$$

Finally, with the result of eq 21, the volume averaged LVRPA (in this case, for the one-dimensional−one-directional model) is

$$\left\langle e^a_{TiO_2,\Sigma\lambda}(x) \right\rangle_{L_R} = \frac{1}{L_R} \int_{L_R} e^a_{TiO_2,\Sigma\lambda}(x)\, dx \qquad (22)$$

With eqs 9, 10, 18, and 22 we can calculate $\eta^{Hom}_{t,\lambda}$ and $\eta^{Het}_{t,\Sigma\lambda}$.

Results and Discussion

Figure 4a illustrates the evolution of the DCA concentration as a function of the effective reaction time for the homogeneous system employing the 40 W lamps (H_2O_2/UV^{40W}) and the 15 W lamps (H_2O_2/UV^{15W}). Figure 4b shows results for the heterogeneous process. The fastest degradation rate was obtained with the H_2O_2/UV^{40W} system, followed by H_2O_2/UV^{15W}. Although the photocatalytic process was effective to degrade DCA, the reaction rate was much slower when compared with the homogeneous processes.

Results employing the comparison criteria previously described are reported in Table 2. For the H_2O_2/UV^{40W} reaction, the DCA conversion at $t_{eff} = 530$ s (ca. 4 h of reaction) is more than 80%, whereas the H_2O_2/UV^{15W} system reaches half of this value. Conversion with TiO_2/UV represents about 10% of the value obtained with H_2O_2/UV^{40W}. If we analyze each process individually, DCA and TOC conversion values are similar. This is in agreement with the fact that there are no stable reaction intermediates and DCA is rapidly converted into HCl and CO_2 (*10, 12*).

Regarding the quantum efficiencies, the corresponding values for H_2O_2/UV employing different lamps are alike. However, for TiO_2/UV, $\eta_{\Sigma\lambda}$ remains low but in the order of the reported efficiencies for photocatalysis (*29, 35*).

The specific energy consumptions of the remediation processes analyzed, as defined in eq 3, are also shown in Table 2. The TiO_2/UV system is again the less convenient process with the highest value of E_S. A possible explanation to this result can be found in the strong radiation absorption by the TiO_2 particles. At a catalyst concentration of 1.0×10^{-3} g cm^{-3}, radiation penetrates the reaction space just a few millimeters and more than 90% of the reactor remains dark, i.e., the oxidation process only takes place in the space adjacent to the reactor windows. More comparable results between both processes can be obtained employing a thinner reactor. The photocatalytic reactor described in the Experimental Setups and Procedures section has a special mechanism of mobile windows that allows the modification of the reactor length L_R (*45*). Table 3 shows results of E_S for the homogeneous (40 W) and heterogeneous systems, for two reactor lengths: 1.0 and 5.0 cm. To calculate E_S, additional photocatalytic experiments were performed employing a reactor length of 1 cm. On the other hand, for the homogeneous process, the value of E_S with $L_R = 1$ cm was obtained theoretically employing a kinetic model for DCA degradation previously validated (*13*). As can be observed from the data reported in Table 3, the E_S for both processes increases when reducing L_R. However, the change is more significant for the H_2O_2/UV^{40W} operation (from 3.35 to 12.2 W s kg^{-1}). As a consequence, for $L_R = 1$ cm, the specific energy consumption for the homogeneous system is similar to the one corresponding to the heterogeneous process.

TABLE 2. Comparison Results

process	DCA conversion (%)	TOC conversion (%)	quantum efficiency (% mol DCA einstein^{-1})	quantum efficiency (% mol TOC einstein^{-1})	specific energy consumption $E_s \times 10^{-10}$ (W s kg^{-1} TOC)
H_2O_2/UV^{40W}	81.4	72.8	17.9	17.2	3.35
H_2O_2/UV^{15W}	42.2	42.3	18.7	18.6	3.50
TiO_2 UV	7.6	8.4	2.4	2.4	11.2

TABLE 3. Specific Energy Consumption for Different Reactor Lengths

	specific energy consumption $E_s \times 10^{-10}$ (W s kg^{-1} TOC)	
process	$L_R = 1$ cm	$L_R = 5$ cm
H_2O_2/UV^{40W}	12.2	3.35
TiO_2/UV	15.8	11.2

With the use of the defined comparison criteria, from the above figures and for the adopted model compound (DCA), it is clear that the performance of the H_2O_2/UV process is much better than that of photocatalysis.

It is clear that one must be very careful concerning the economics of both processes and that in "typical" situations the results may differ substantially from those obtained in this study made under "optimal" conditions. Definitely, the cost of hydrogen peroxide which, in addition, cannot make use of solar radiation, will be higher than the cost of titanium dioxide as long as the catalyst is stable; i.e., its life, as it happens in many circumstances, is very long. Some titanium dioxide varieties are very effective in slurry operations. Under these conditions, there are only two drawbacks: (1) the fouling of the reactor walls is very significant, a factor that affects the radiation entrance to the reactor and is seldom mentioned, and (2) when the particulate catalyst is used, one must consider the post-treatment catalyst separation costs. Immobilized catalysts in waters systems do not have the same efficiency and have other problems concerning mechanical stability and/or mass transfer limitations. Finally, when waters or wastewaters have very low radiation transmission characteristics, both processes have difficulties, as in any photochemical reaction, the case of hydrogen peroxide being worse, due to the low absorption coefficient as compared with titanium dioxide to compete for the entering photons. For practical applications, and particularly when the operating conditions are variable, the analysis must be made in other terms. It is very likely that in those cases, the performance of titanium dioxide may be more robust.

These results are, additionally, an indication that most of the research efforts should be aimed at improving the catalyst performance in all the above-mentioned aspects. Different strategies have already been proposed to enhance the photoactivity of TiO_2. Among the most interesting ap-

proaches, we can cite the doping of the semiconductor with metals to obtain a double effect (*46*): (i) the decrease of the electron−hole recombination rate and the resulting loss of energy as heat; (ii) the shift of the absorption band to the visible region to increase the utilization of solar light and, therefore, to reduce the costs of electrical energy.

Acknowledgments

The authors are grateful to Universidad Nacional del Litoral (UNL), Consejo Nacional de Investigaciones Cientı´ficas y Técnicas (CONICET), and Agencia Nacional de Promoción Cientı´fica y Tecnológica (ANPCyT) for the financial support. They also thank Antonio C. Negro for his valuable help during the experimental work and Claudia M. Romani for technical assistance.

Appendix A

NOMENCLATURE

C	molar concentration, mol cm^{-3}
C_m	catalyst mass concentration, g cm^{-3}
e^a	local volumetric rate of photon absorption, einstein cm^{-3} s^{-1}
E_S	specific energy consumption, W s kg^{-1}
G	incident radiation, einstein cm^{-2} s^{-1}
g	asymmetry factor, dimensionless
I	radiation intensity, einstein cm^{-2} sr^{-1} s^{-1}
$\bar{I}$	intensity in the one-dimensional, single-directional radiation model, einstein cm^{-3} s^{-1}
j^e	rate of photon emitted per unit volume and solid angle, einstein cm^{-3} sr^{-1} s^{-1}
L	length, cm
n	refractive index, dimensionless
p	phase function, dimensionless
R	reaction rate, mol cm^{-3} s^{-1}
r	initial molar ratio between H_2O_2 and DCA
t	time, s
t_{eff}	effective reaction time, s
V	volume, cm^3 or m^3
x	axial coordinate, cm
x	position vector, cm

Greek Letters

ε_L	liquid holdup, dimensionless
β	volumetric extinction coefficient, cm^{-1}
Γ	compound reflection function, dimensionless
θ	spherical coordinate, rad
θ_c	critical angle, rad
κ	volumetric absorption coefficient, cm^{-1}
λ	radiation wavelength, nm
μ	direction cosine of the ray for which the RTE is written
μ'	direction cosine of an arbitrary ray before scattering
μ_c	cosine of the critical angle θ_c
σ	volumetric scattering coefficient, cm^{-1}
η_λ	quantum yield, mol einstein^{-1}
$\eta_{\Sigma\lambda}$	quantum efficiency, mol einstein^{-1}
Ω	solid angle, sr
Ω'	unit vector in the direction of radiation propagation, dimensionless

Subscripts

a	air
DCA	dichloroacetic acid
i	DCA or TOC
L_R	relative to the reactor window at $x = L_R$
R	reactor
s	suspension
T	total system
Tk	tank
TOC	total organic carbon
W	reactor window
0	initial condition; also, relative to the reactor window at $x = 0$
λ	dependence on wavelength

Superscripts

Het	heterogeneous reaction
Hom	homogeneous reaction
0	initial condition

Special Symbols

$\langle\ \rangle$	denotes average value over a given space

Supporting Information Available

Brief derivation of the equations employed in the radiation model, including the definition of the variables and simplifications for the systems under study. This material is available free of charge via the Internet at http://pubs.acs.org.

Literature Cited

(1) Kaneko, M.; Okura, I. *Photocatalysis: Science and Technology*; Kodansha Springer: Tokyo, Berlin, 2002.

(2) Pichat, P. Photocatalytic degradation of pollutants in water and air: Basic concepts and applications. In *Chemical Degradation Methods for Wastes and Pollutants: Environmental and Industrial Applications*; Tarr, M. A., Ed.; Marcel Dekker: New York/Basel, 2003; pp 77−119.

(3) Agrios, A. G.; Pichat, P. State of the art and perspectives on materials and applications of photocatalysis over TiO_2. *J. Appl. Electrochem.* **2005**, *35*, 655–663.

(4) Beltran, F. J. Ozone−UV radiation−hydrogen peroxide oxidation technologies. In *Chemical Degradation Methods for Wastes and Pollutants: Environmental and Industrial Applications*; Tarr, M. A., Ed.; Marcel Dekker: New York/Basel, 2003; pp 1−75.

(5) Benitez, F. J.; Real, F. J.; Acero, J. L.; Garcia, C. Photochemical oxidation processes for the elimination of phenyl-urea herbicides in waters. *J. Hazard. Mater.* **2006**, *B138*, 278–287.

(6) Yonar, T.; Kestioglu, K.; Azbar, N. Treatability studies on domestic wastewater using UV/H_2O_2 process. *Appl. Catal., B* **2006**, *67*, 223–228.

(7) Pérez-Estrada, L. A.; Malato, S.; Gernjak, W.; Agüera, A.; Thurman, E. M.; Ferrer, I.; Fernández-Alba, A. R. Photo-fenton degradation of diclofenac: Identification of main intermediates and degradation pathway. *Environ. Sci. Technol.* **2005**, *39*, 8300–8306.

(8) Pignatello, J. J.; Oliveros, E.; MacKay, A. Advanced oxidation processes for organic contaminant destruction based on the Fenton reaction and related chemistry. *Crit. Rev. Environ. Sci. Technol.* **2006**, *36*, 1–84.

(9) Gernjak, W.; Fuerhacker, M.; Fernández-Ibañez, P.; Blanco, J.; Malato, S. Solar photo-Fenton treatment-process parameters and process control. *Appl. Catal., B* **2006**, *64*, 121–130.

(10) Zalazar, C. S.; Martı´n, C. A.; Cassano, A. E. Photocatalytic intrinsic reaction kinetics. II: Effects of oxygen concentration on the kinetics of the photocatalytic degradation of dichloroacetic acid. *Chem. Eng. Sci.* **2005**, *60*, 4311–4322.

(11) Zalazar, C. S.; Romero, R. L.; Martı´n, C. A.; Cassano, A. E. Photocatalytic intrinsic reaction kinetics. I: Mineralization of dichloroacetic acid. *Chem. Eng. Sci.* **2005**, *60*, 5240–5254.

(12) Zalazar, C. S.; Labas, M. D.; Brandi, R. J.; Cassano, A. E. Dichloroacetic acid degradation employing hydrogen peroxide and UV radiation. *Chemosphere* **2007**, *66*, 808–815.

(13) Zalazar, C. S.; Lovato, M. E.; Labas, M. D.; Brandi, R. J.; Cassano, A. E. Intrinsic kinetics of the oxidative reaction of dichloroacetic acid employing hydrogen peroxide and ultraviolet radiation. *Chem. Eng. Sci.* **2007**, *62*, 5840–5853.

(14) Sakthivel, S.; Hidalgo, M. C.; Bahnemann, D. W.; Geissen, S.-U.; Murugesan, V.; Vogelpohl, A. A fine route to tune the photocatalytic activity of TiO2. *Appl. Catal., B* **2006**, *63*, 31–40.

(15) Enriquez, R.; Agrios, A. G.; Pichat, P. Probing multiple effects of TiO2 sintering temperature on photocatalytic activity in water by use of a series of organic pollutant molecules. *Catal. Today* **2007**, *120*, 196–202.

(16) Hirvonen, A.; Tuhkanen, T.; Kalliokoski, P. Formation of chlorinated acetic acids during UV/H_2O_2-oxidation of ground water contaminated with chlorinated ethylenes. *Chemosphere* **1996**, *32*, 1091–1102.

(17) Brandi, R. J.; Alfano, O. M.; Cassano, A. E. Rigorous model and experimental verification of the radiation field in a flat-plat solar collector simulator employed for photocatalytic reactions. *Chem. Eng. Sci.* **1999**, *54*, 2817–2827.
(18) Allen, A.; Hochanadel, C.; Ghormley, J.; Davis, T. Decomposition of water and aqueous solutions under mixed fast neutron and γ radiation. *J. Phys. Chem.* **1952**, *56*, 575–586.
(19) Montgomery Watson Harza (MWH). *Water Treatment. Principles and Design*, 2nd ed.; John Wiley & Sons: New York, 2005.
(20) Crittenden, J.; Hu, S.; Hand, D.; Green, S. A kinetic model for H_2O_2/UV process in a completely mixed batch reactor. *Water Res.* **1999**, *33*, 2315–2328.
(21) Gogate, P.; Pandit, A. A review of imperative technologies for wastewater treatment II: hybrid methods. *Adv. Environ. Res.* **2004**, *8*, 553–597.
(22) Ballari, M. d. l. M.; Brandi, R. J.; Alfano, O. M.; Cassano, A. E. Mass transfer limitations in photocatalytic reactors employing titanium dioxide suspensions I. Concentration profiles in the bulk. *Chem. Eng. J.* **2008**, *136*, 242–255.
(23) Zalazar, C. S.; Labas, M. D.; Martín, C. A.; Brandi, R. J.; Alfano, O. M.; Cassano, A. E. The extended use of actinometry in the interpretation of photochemical reaction engineering data. *Chem. Eng. J.* **2005**, *109*, 67–81.
(24) Braun, A. M.; Maurette, M. T.; Oliveros, E. *Photochemical Technology*; Wiley: New York, 1991.
(25) Palmisano, L.; Augugliaro, V.; Campostrini, R.; Schiavello, M. A. Proposal for the quantitative assessment of heterogeneous photocatalytic processes. *J. Catal.* **1993**, *143*, 149–154.
(26) Sun, L.; Bolton, J. R. Determination of the quantum yield for the photochemical generation of hydroxyl radicals in TiO_2 suspensions. *J. Phys. Chem.* **1996**, *100*, 4127–4134.
(27) Serpone, N. Relative photonic efficiencies and quantum yields in heterogeneous photocatalysis. *J. Photochem. Photobiol., A* **1997**, *104*, 1–12.
(28) Cabrera, M. I.; Alfano, O. M.; Cassano, A. E. Quantum efficiencies of the photocatalytic decomposition of trichloroethylene in water. A comparative study for different varieties of titanium dioxide catalysts. *J. Adv. Oxid. Technol.* **1998**, *3*, 220–228.
(29) Salaices, M.; Serrano, B.; de Lasa, H. I. Photocatalytic conversion of organic pollutants. Extinction coefficients and quantum efficiencies. *Ind. Eng. Chem. Res.* **2001**, *40*, 5455–5464.
(30) Salaices, M.; Serrano, B.; de Lasa, H. I. Experimental evaluation of photon absorption in an aqueous TiO_2 slurry reactor. *Chem. Eng. J.* **2002**, *90*, 219–229.
(31) Curcó, D.; Giménez, J.; Addardak, A.; Cervera-March, S.; Esplugas, S. Effects of radiation absorption and catalyst concentration on the photocatalytic degradation of pollutants. *Catal. Today* **2002**, *76*, 177–188.
(32) Brandi, R. J.; Citroni, M. A.; Alfano, O. M.; Cassano, A. E. Absolute quantum yields in photocatalytic slurry reactors. *Chem. Eng. Sci.* **2003**, *58*, 979–985.
(33) Yokota, T.; Cesur, S.; Suzuki, H.; Baba, H.; Takahata, Y. Anisotropic scattering model for estimation of light absorption rates in a photoreactor with heterogeneous medium. *J. Chem. Eng. Jpn.* **1999**, *32*, 314–321.
(34) Yang, Q.; Ang, P. L.; Ray, M. B.; Phekonen, S. O. Light distribution field in catalyst suspensions within an annular photoreactor. *Chem. Eng. Sci.* **2005**, *60*, 5255–5268.
(35) Satuf, M. L.; Brandi, R. J.; Cassano, A. E.; Alfano, O. M. Quantum efficiencies of 4-chlorophenol photocatalytic degradation and mineralization in a well-mixed slurry reactor. *Ind. Eng. Chem. Res.* **2007**, *46*, 43–51.
(36) Imoberdorf, G. E.; Cassano, A. E.; Irazoqui, H. A.; Alfano, O. M. Simulation of a multi-annular photocatalytic reactor for degradation of perchloroethylene in air: Parametric analysis of radiative energy efficiencies. *Chem. Eng. Sci.* **2007**, *64*, 1138–1154.
(37) Satuf, M. L.; Brandi, R. J.; Cassano, A. E.; Alfano, O. M. Experimental method to evaluate the optical properties of aqueous titanium dioxide suspensions. *Ind. Eng. Chem. Res.* **2005**, *44*, 6643–6649.
(38) Badawy, M. I.; Ghaly, M. Y.; Gad-Allah, T. A. Advanced oxidation processes for the removal of organophosphorus pesticides from wastewater. *Desalination* **2006**, *194*, 166–175.
(39) Labas, M. D.; Zalazar, C. S.; Brandi, R. J.; Martı´n, C. A.; Cassano, A. E. Scaling-up of a photoreactor for formic acid degradation employing hydrogen peroxide and UV radiation. *Helv. Chim. Acta* **2002**, *85*, 82–95.
(40) Cabrera, M. I.; Negro, A. C.; Alfano, O. M.; Cassano, A. E. Photocatalytic reactions involving hydroxyl radical attack. II. Kinetics of the decomposition of trichloroethylene using titanium dioxide. *J. Catal.* **1997**, *172*, 380–390.
(41) Martín, C. A.; Alfano, O. M.; Cassano, A. E. Decolorization of water for domestic supply employing UV radiation and hydrogen peroxide. *Catal. Today* **2000**, *60*, 119–127.
(42) Alfano, O.; Negro, A.; Cabrera, M.; Cassano, A. Scattering effects produced by inert particles in photochemical reactors. 1. Model and experimental verification. *Ind. Eng. Chem. Res.* **1995**, *34*, 488–499.
(43) Siegel, R.; Howell, J. *Thermal Radiation Heat Transfer*, 4th ed.; Hemisphere Publishing Corp.: Bristol, PA, 2002.
(44) Duderstadt, J.; Martin, R. *Transport Theory*; Wiley: New York, 1979.
(45) Satuf, M. L.; Brandi, R. J.; Cassano, A. E.; Alfano, O. M. Scaling-up of slurry reactors for the photocatalytic degradation of 4-chlorophenol. *Catal. Today* **2007**, *129*, 110–117.
(46) Colmenares, J. C.; Aramendı´a, M. A.; Marinas, A.; Marinas, J. M.; Urbano, F. J. Synthesis, characterization and photocatalytic activity of different metal-doped titania systems. *Appl. Catal., A* **2006**, *306*, 120–127.

ES800028H